Journal of Nuclear Materials 401 (2010) 118–123

Contents lists available at ScienceDirect

Journal of Nuclear Materials

journal homepage: www.elsevier.com/locate/jnucmat

First-principles study of the electronic structure and optical properties of UO_2

Qiuyun Chen, Xinchun Lai *, Tao Tang, Bin Bai, Mingfu Chu, Yongbin Zhang, Shiyong Tan

National Key Laboratory for Surface Physics and Chemistry, P.O. Box 718-35, Mianyang 621907, Sichuan, China

ARTICLE INFO

Article history:
Received 3 November 2009
Accepted 12 April 2010

ABSTRACT

We present first-principles calculations of the electronic structure and optical properties for UO_2 based on density-functional theory using the generalized gradient approximation (GGA). Hubbard *U* correction is employed to treat the strong correlation 5f electrons. The calculated lattice parameters and band gap are in good agreement with the experimental data. Furthermore, the dielectric function and the optical properties, such as reflectivity, refractive index, extinction coefficient, energy-loss spectrum and absorption coefficient are derived and analyzed. The calculated results are compared with the experimental data from both published literatures and our own results.

1. Introduction

Uranium dioxide (UO_2) is the standard fuel utilized in light water nuclear reactors, and it is widely used in nuclear industry. Analysis shows that depleted uranium is a promising material for mirror coatings in the soft X-ray range and the EUV (extreme ultra-violet) region, and uranium thin films can be used in applications such as space telescopes and in multilayer mirrors [1–4]. Unfortunately, these thin films are highly unstable due to the rapid oxidation of uranium upon removal from vacuum. This instability in uranium thin films has led to increased interest in uranium oxide thin films because of their stability and high reflectivity in some region of wavelength [2,3]. Experimentally, the optical properties of uranium-based mirrors have been studied since the early 1990s by different research teams [2–11]. However, at present there is no theoretical report about optical properties of the bulk UO_2. Exploring the electronic and optical properties of UO_2 should have important signification to improve the range of practical applications. Furthermore, it can provide interpretations for experimental data.

The electronic structure of UO_2 has been the subject of theoretical investigations over the last 30 years. Also, many theoretical studies have contributed to understanding the behavior of fission products (Xe, Kr, I, etc.) and He in various defects of UO_2 [12–18]. However, some questions concerning correct description of their insulating properties are still unclear. Some approaches were used to remedy the band gap problem. Some research teams [15–17] used GGA + *U* or LDA + *U* method and succeeded in predicting UO_2 to be a semi-conductor, or even insulator; others [19] used *hybrid* density-functional theory (DFT), and correctly yielded an anti-ferromagnetic insulator.

In this paper, we present a detailed investigation on the geometries, electronic structure and optical properties of UO_2 using the first-principles method within generalized gradient approximation (GGA), and Hubbard *U* correction term is taken into account. We investigate the optical properties, including the frequency-dependent dielectric function, reflectivity, refractive index, extinction coefficient, energy-loss spectrum and absorption coefficient. Comparison is made between our calculated results and the available experimental results from both published literatures and our own experiments.

2. Models and methods

The results described below were based on density function theory, as implemented in CASTEP code which uses a plane wave basis set for expansion of effective single particle Kohn–Sham energy [20,21]. Ultra-soft pseudo-potentials were used to describe the interactions of ionic core and valence electrons. We used standard GGA approaches for the exchange–correlation functional in calculating of all the properties (cell parameters, band structure, density of states and optical properties), Hubbard *U* correction term is taken into account. It provides good ground-state properties of UO_2 and other strongly correlated systems, *e.g.* transition metal oxides, including the band gap and magnetic properties [22,23]. In particular, the advantage of this DFT + *U* version is that the correlation (*U*) and exchange (*J*) parameters do not enter separately the Hamiltonian; only the difference *U*–*J* is essential. In our calculation, only one parameter (*U*) is adjustable. In order to obtain the best *U* value, we used one of the methods Mosey [24] recommended. We have tried various values of *U* and found that choice

* Corresponding author.
E-mail address: lai319@yahoo.com (X. Lai).

0022-3115/$ - see front matter © 2010 Elsevier B.V. All rights reserved.
doi:10.1016/j.jnucmat.2010.04.007

of $U = 4.1$ eV leads to best agreement between the data observed experimentally and simulated using ab initio methods.

The UO_2 crystal can be described by the fluorite structure, depending on the crystallographic definition of the space group Fm-3 m (No. 225) [25]. Here we used the experimental lattice constants ($a = b = c = 5.468$ Å) as the initial parameter for the geometry optimization of the unit cell. The valence atomic configurations are $6s^2 6p^6 7s^2 5f^2 6d^2$ for U atom, $2s^2 2p^4$ for O atom. Spin polarization is considered in the calculations. Energy calculations in the first irreducible Brillouin zone were performed using a special k-point sampling methods of Monkhorst–Pack scheme. Broyden–Fletcher–Goldhaber–Shanno (BFGS) optimization method [26] was used to find the ground state of UO_2 crystals in which both atom positions and lattice parameters were optimized simultaneously. Total energy changes were finally reduced less than 2×10^{-6} eV/atom, and Hellman–Feynman forces acting on atoms were converged less than 0.05 eV/Å. In order to get the precise crystal structures and total energies, all structural degrees of freedom including unit-cell volume and shape as well as atomic positions are relaxed simultaneously.

3. Results and discussion

3.1. Crystalline structure optimization

Since the accuracy of the first-principle calculations may be dependent on many parameters, such as kinetic energy cut off value for plane wave expansions, exchange–correlation energy scheme and k-point grid, etc. We calculated the variations of optimized cell parameters and final bulk modulus as a function of energy cut-off values, the GGA within PBE and PW91 schemes are both used in order to assure the accuracy of our results. We also checked the convergence regarding different k-point sampling grid.

As shown in Fig. 2, at every cut-off energy the calculated optimized cell parameters from PW91 is much higher than that from PBE, the variation tendency is similar. On the other hand, we can see the fluctuation of final bulk modulus above the cut-off energy of 450 eV. From Fig. 2, we can conclude that a kinetic energy cut-off 400 eV was sufficient for plane wave expansions in reciprocal space of UO_2. Fig. 3 shows the variation of optimized cell parameters and final bulk modulus of UO_2 regarding different k-point sam-

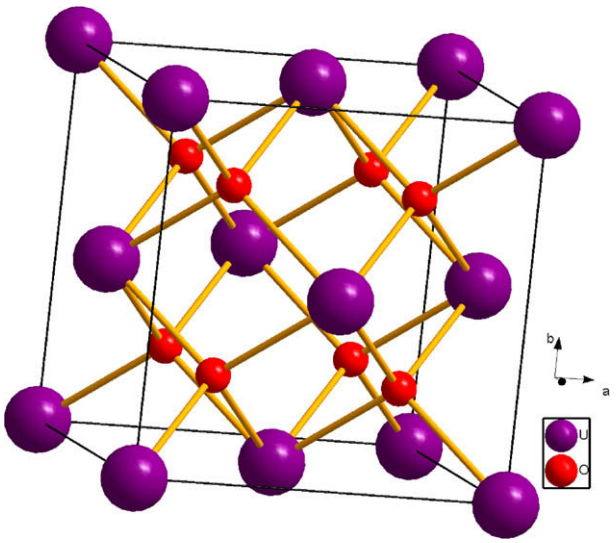

Fig. 1. The unit cell of UO_2 crystal. The smaller (red) and larger (purple) balls represent O and U, respectively. (For interpretation of the references to colour in this figure legend, the reader is referred to the web version of this article.)

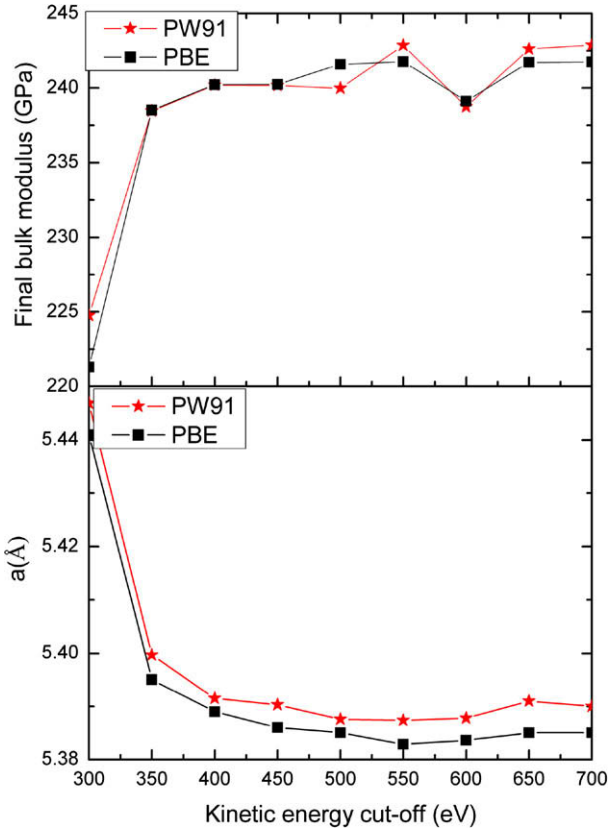

Fig. 2. The variation of optimized cell parameters and final bulk modulus of UO_2 as a function of energy cut-off values, both PBE and PW91 were used and compared.

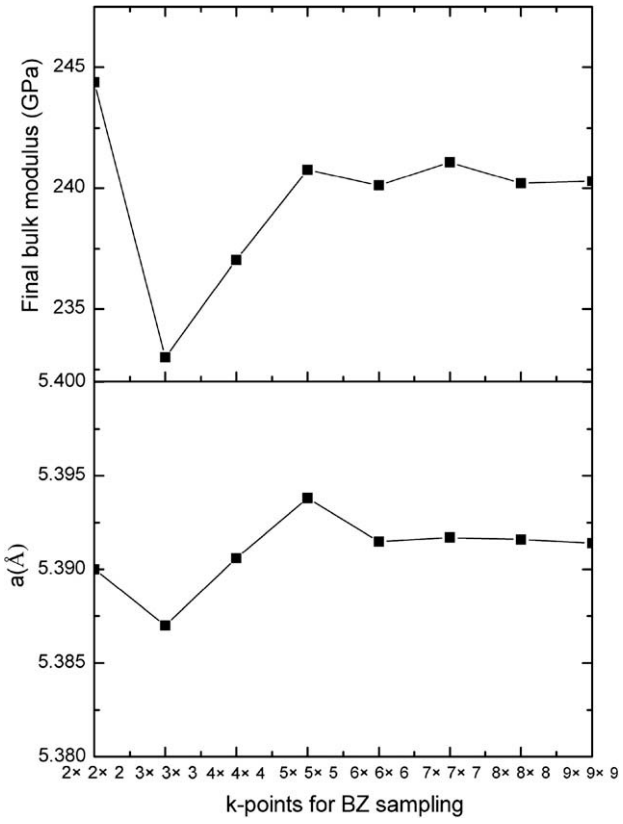

Fig. 3. The variation of optimized cell parameters and final bulk modulus of UO_2 regarding different k-point sampling grid.

Table 1
The calculated lattice parameters and band gap of bulk uranium dioxide. Results of our work are compared with published experimental and theoretical data. It is noted that the lattice parameter was reported at room temperature while the ab initio calculation data are determined at 0 K.

	Method	Lattice parameter (Å)	Band gap (eV)
Experiment [6]		5.47	2.1 ± 0.1
Dudarev et al. [22]	LMTO-LSDA + *U*	5.37	1.3
Gupta et al. [16]	PAW-SP-GGA + *U*	5.55	1.8
Nerikar et al. [17]	PAW-SP-GGA + *U*	5.49	1.92
	SP-GGA	5.42	0
	LDA	5.26	0
Our work	GGA + *U*	5.39	1.87

pling grid. From Fig. 3 we can see that there is slight change when the *k*-point sampling grid is more than $6 \times 6 \times 6$, so $6 \times 6 \times 6$ *k*-point grid is sufficient. The calculated bulk modulus is 240 Gpa, a value that is about 12% larger than the experimental value [13].

Furthermore, we calculated the band gap of UO_2. The results are compared with the published computational and experimental values, which were illustrated in Table 1. From Table 1, it is found that the extent of agreement with the experimental lattice parameter improves with proper selected approximations. For example, pure LDA and GGA calculations agree badly with experimental results, but improve with the consideration of spin polarization. The band gap of our results using GGA + *U* is very close to that of Gupta's, but still a little lower than experimental results.

3.2. Electronic structures of UO_2 crystals

Uranium dioxide is an electrical insulator. However, DFT predicts it to be a metal unless the 5f electron on site repulsion is included using the *U* term. Fig. 4 shows the band structure of UO_2 calculated from GGA + *U* methods. It gives a band gap of 1.87 eV, which is only 0.23 eV smaller than the experimental value. Fig. 5 shows the total and partial density of states (DOS) of UO_2 crystals. The Fermi energy was assumed to be zero energy level. More detailed analysis show that the valence band consists mainly of U 5f and O 2p orbitals, while the conduction band is mainly derived from U 6d and U 5f orbitals. This correct description of the electronic state shows that the method can be used to describe the optical properties of uranium dioxide.

3.3. Optical properties of UO_2 crystals

It is known that the dielectric function is mainly related with the electronic response. The imaginary part $\varepsilon_2(\omega)$ of the dielectric

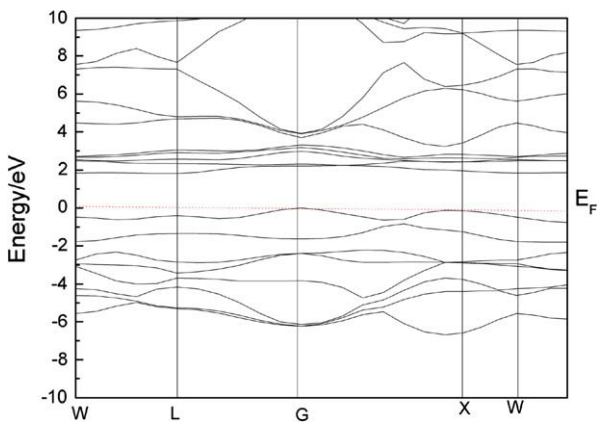

Fig. 4. Band structure of UO_2. The Fermi level is indicated by a dotted line.

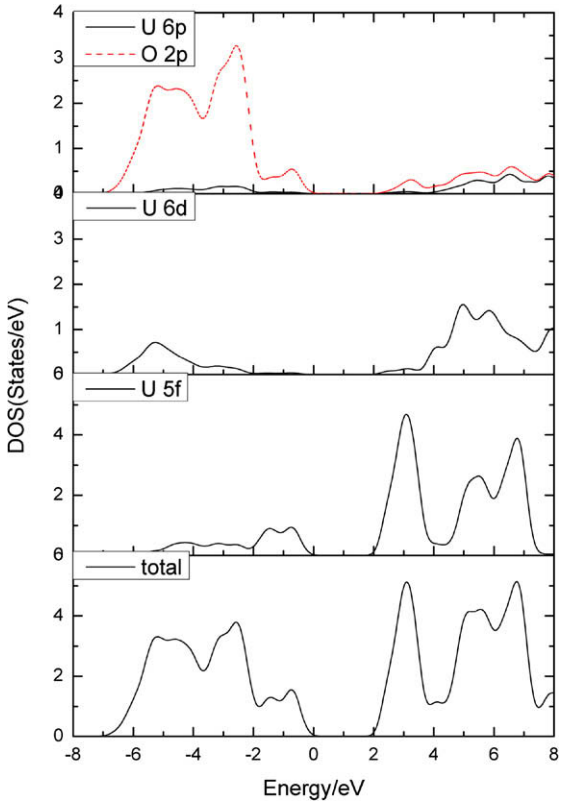

Fig. 5. Calculated total and partial density of states (DOS) in the crystal of UO_2.

function $\varepsilon(\omega)$ is calculated from the momentum matrix elements between the occupied and unoccupied wave functions, given by Ref. [27]

$$\varepsilon_2 = \frac{\upsilon e^2}{2\pi\hbar m^2\omega^2}\int d^3k \sum_{n,n'} \left|\langle kn|p|kn'\rangle\right|^2 \times f(kn)(1-f(kn'))\delta(E_{kn}-E_{kn'}-\hbar\omega) \tag{1}$$

where $\hbar\omega$ is the energy of the incident photon, p is the momentum operator $(\hbar/i)(\partial/\partial_x)$, $(|kn\rangle)$ is a crystal wave function, and $f(kn)$ is the Fermi function. The real part $\varepsilon_1(\omega)$ of the dielectric function $\varepsilon(\omega)$ is evaluated from imaginary part $\varepsilon_2(\omega)$ by the Kramer–Kronig transformation. The absorption coefficient $I(\omega)$ can be derived from $\varepsilon_1(\omega)$ and $\varepsilon_2(\omega)$ by [27]

$$I(\omega) = \sqrt{2}\omega\left[\sqrt{\varepsilon_1^2(\omega)+\varepsilon_2^2(\omega)} - \varepsilon_1(\omega)\right]^{1/2} \tag{2}$$

All other optical constants can also be obtained; they depend on $\varepsilon_1(\omega)$ and $\varepsilon_2(\omega)$ and thus on the energy. Now we can explore the optical properties of UO_2.

From the electronic structures, the optical properties of UO_2 have been calculated. In Fig. 6 we show the calculated imaginary parts of the dielectric function ε_ω for UO_2 crystals in the energy range of 0–14 eV. Inset is the picture of the experimental results obtained by Schoenes [6] in the energy range of 0–13 eV.

The imaginary part ε_2 of dielectric function is directly connected with the energy band structure. From Fig. 6a we can see that the value of ε_2 starts from about 1.9 eV, and it is in accordance with the value of band gap described above. It also indicates the underestimation of band gap. The first peak displays a maximum at 3.5 eV and a shoulder at 5.5 eV. The following two main peaks appear at 8.4 eV and 10.8 eV, respectively. A small peak appears at 13.0 eV. Schoenes [6] shows that the first peak of the experimental value appeared at 3.05 eV, two main peaks appear at 7.95 eV and

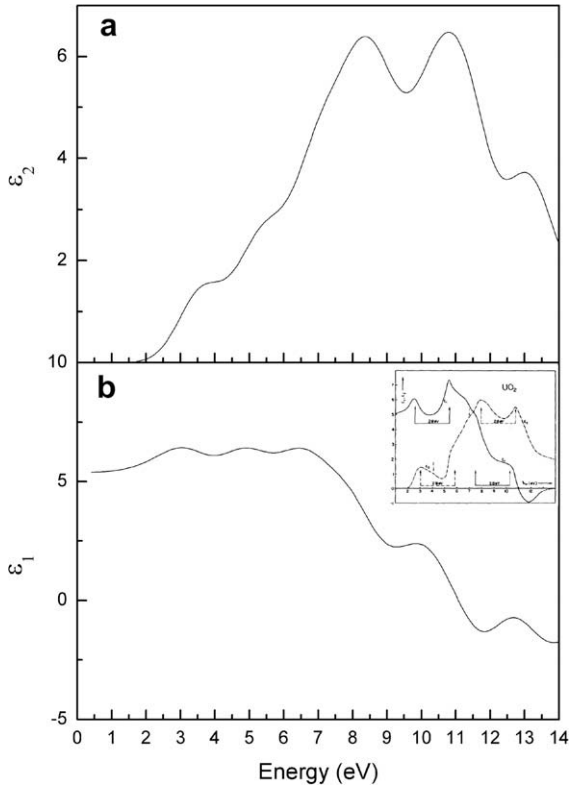

Fig. 6. The real part (ε_1 and imaginary part (ε_2) of the dielectric function ε_ω for UO_2.

10.75 eV. The difference between two main peaks was 2.8 eV. It was thought that the cubic environment of the uranium ions splits the 6d band into two sub-bands, which caused the separation of the two peaks, and the value was 2.8 eV. The indicated width of the two peaks 8.4 eV and 10.8 eV in this work is 2.4 eV, which is 0.4 eV less compared with the result of Schoenes' experiment. The two major peaks at 7.95 eV and 10.75 eV in ε_2 are thought to be due to charge transfer transitions from a valence band formed by 2p states of oxygen to 6d band in Ref. [6], we agree with this conclusion. But from our density of states calculation shown in Fig. 5, the situation is much more complicated than energy levels drawn in Fig. 3 of Ref. [6], which was concluded from measurement of reflectivity. The comparison between our result of $\varepsilon_1(\omega)$ and $\varepsilon_2(\omega)$ and with that of experimental ones show that the major characters are close, but there are two major differences. First, there is about 0.5 eV red shift between experimental and calculated results in low energy region, which we think is caused by the different temperature of the two cases, the calculation is done at 0 K, while the experiment was done at 300 K. The second difference is that in low energy region the experimental peaks are more pronounced than calculated ones. The cause of this difference may be that the experimental sample is not perfect crystal UO_2 and impurity exists that makes absorption easier and stronger, and high temperature (300–0 K) intensifies this trend. Another possibility is that in our calculation spin orbit coupling effects was underestimated.

Fig. 7 shows the variations of reflectivity of UO_2 in the energy range of 0–14 eV. The comparison was made between our calculated results and the experimental results by Schoenes [6]. From Fig. 6 we can see that the first peak displays a maximum at 2.8 eV, and the following three peaks appear at 5.0 eV, 8.1 eV, and 11.3 eV, respectively. In Schoenes' work, the first peak appears at 2.6 eV, and the following three peaks appear at 5.5 eV, 8 eV and 11.7 eV, respectively. The reflectance of first four peaks 2.8 eV,

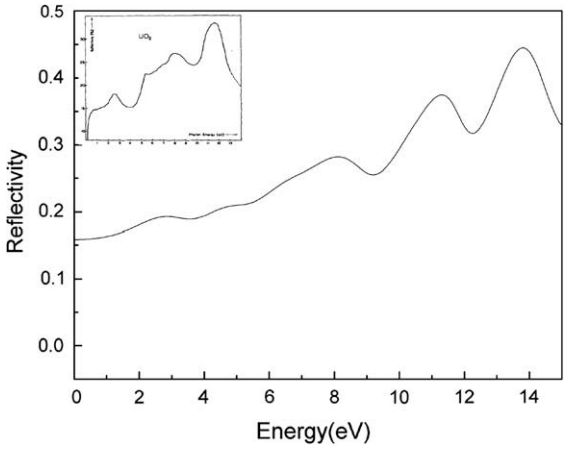

Fig. 7. Calculated reflectivity of UO_2 as a function of energy. The inset is the reflectivity for UO_2 single crystal from experimental results by Schoenes [6].

5.0 eV, 8.1 eV, 11.3 eV of our calculation is 19%, 22%, 28% and 37%, respectively, which is close to the experimental value (judged from Fig. 1 of Schoenes' work) ~18%, 23%, 27% and 33%, respectively. The reflectance of peak 13.8 eV in Fig. 7 reaches a reflectance of 45%. Above 13.8 eV, the reflectance drops strongly. We can see that our results of the reflectivity agree with experimental results pretty well bellow photon energy 13 eV by peak position and shape. But there is difference between our results and experimental ones. The major difference is that in our result there is a peak at 13.8 eV, while in Schoenes' work there is no such a peak. We'd like to point out that the first-principle calculations were performed at 0 K of perfect crystal, while the experimental results by Schoenes [6] were obtained at 300 K of UO_2 [1 1 1] annealed single crystal with unavoidable damage on surface. According to Ref. [6], the measurement was done with photon energy between 0.03 eV and 13 eV, so it is clear that a peak at 13.8 eV is over energy of incidence. Besides that, according to Ref. [6] a decrease caused by surface imperfection in the reflectance as much as 50% could be observed for the highest photon energies, and different annealing temperature can cause change of reflectance in the far ultra-violet region. In summary, it is reasonable that there is no peak around 13.8 eV in Schoenes' work [6].

In our previous work, we prepared UO_2 thin films by magnetron sputtering method [28]. Refractive indices and extinction coefficients were obtained by ellipsometric spectroscopy measurements.

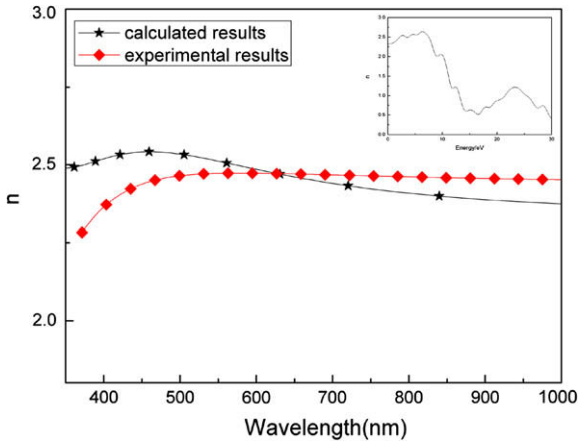

Fig. 8. Calculated refractive index (n) of UO_2 as a function of wavelength, which is compared with our experimental results by ellipsometry. The inset is the calculated refractive index in the energy range from 0 to 30 eV.

In order to further evaluate the accuracy of the GGA + U method used in this work, a comparison was made between our calculated results and experimental results. Figs. 8 and 9 are the comparison of refractive indices and extinction coefficients as a function of wavelength in the range between 350 nm and 1000 nm, respectively.

From Fig. 8, we can see that the calculated values are very close to our experimental results, although some difference exists. At about 628 nm, the value from both methods is the same. The n values below 628 nm from experimental results are much smaller than that of calculated results, and the opposite tendency appears above 628 nm. From Fig. 9, we can see that the k values from experimental results are larger than that from calculated results over the whole wavelength range. However, the shape and trend of both curves are almost the same, and hence the difference between them is acceptable.

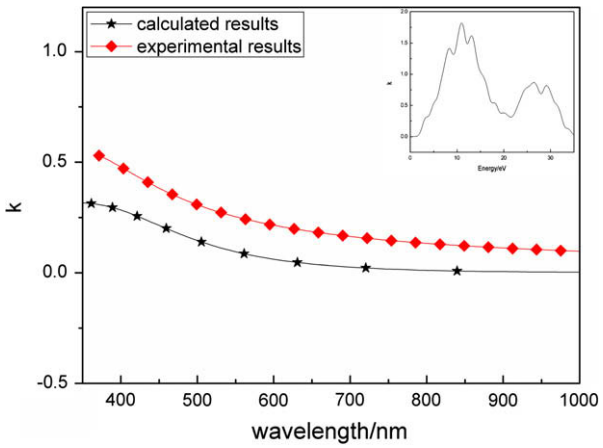

Fig. 9. Calculated extinction coefficients (k) of UO_2 as a function of wavelength, which are compared with our experimental results by ellipsometry. The inset is the calculated extinction coefficient in the energy range from 0 to 30 eV.

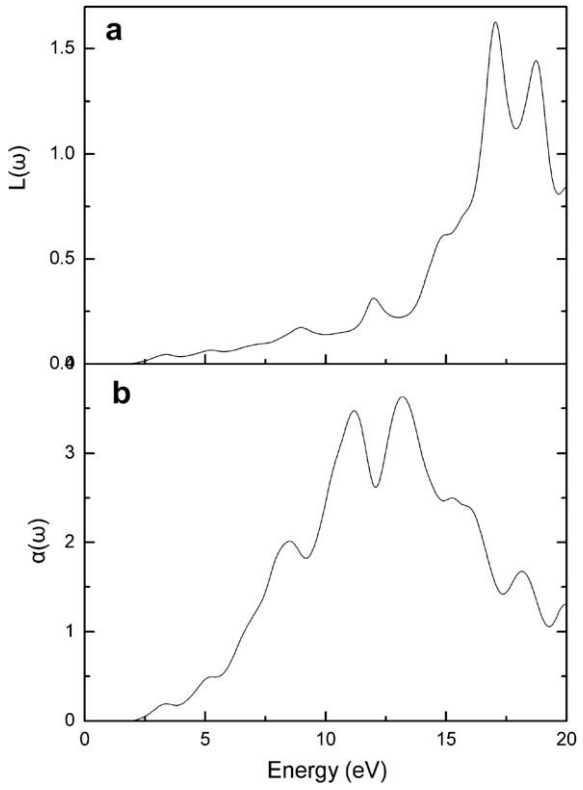

Fig. 10. The calculated optical parameters of UO_2 crystals: (a) energy-loss spectrum, (b) absorption spectrum ($\times 10^5$/cm).

Fig. 10 shows the calculated energy-loss spectrum $L(\omega)$ and absorption spectrum $\alpha(\omega)$ from dielectric functions. The calculated electron energy-loss spectrum $L(\omega)$ describes the energy loss of the fast electron traveling in the material [29]. The peaks of the calculated loss spectrum are at about 12.0 eV, 17 eV, 18.8 eV, which correspond to a rapid decrease of reflectance in Fig. 7. The absorption band $\alpha(\omega)$, covering an energy range of 0–20 eV, shows a very intense absorption occurs between 10 and 15 eV.

4. Conclusions

The geometries, electronic structures and optical properties of UO_2 were calculated using the first-principles method. We employed Hubbard U correction to treat the strong correlation 5f electrons. The comparison was made with the available published experimental results and our own experimental results. Our method gives a band gap of 1.87 eV, which is close to the experimental results. The valence band consists mainly of U 5f and O 2p orbitals, while the conduction band is mainly derived from U 6d and 5f orbitals. The peak positions of both dielectric function and reflectance from GGA + U method is in good agreement with published experimental results. There is slight difference between our experimental results and calculated results, which is acceptable.

Acknowledgements

We are grateful to Peng Shi, Binyun Ao, Li Huang for some instructive suggestions. The project is supported by the Foundations for Development of Science and Technology of China Academy of Engineering Physics (Grant No. 2009B0301037).

References

[1] I.A. Artioukov, R.M. Fechtchenko, A.L. Udovskii, Nucl. Instrum. Meth. Phys. Res. Sect. A 372 (2004) 517.
[2] D.D. Allred, M.B. Squires, R.S. Turley, W. Cash, A. Shipley, Proc. SPIE. 4782 (2002) 12–223.
[3] R.L. Sandberg, D.D. Allred, S. Lunt, Proc. SPIE. 5193 (2003) 191–203.
[4] I.A. Artioukov, O.V. Chefonov, O.N. Gilev, A.V. Lipin, V.I. Oatashev, Nucl. Instrum. Meth. Phys. Res. A 575 (2007) 248–250.
[5] V.A. Pronin, D.A. Vikhlyaev, O.N. Gilev, A.L. Zapysov, A.V. Lipin, Tech. Phys. 53 (2008) 1615–1618.
[6] J. Schoenes, J. Appl. Phys. 49 (1978) 1463.
[7] T.T. Meek, B. von Roedern, Vacuum 83 (2009) 226–228.
[8] T.T. Meek, B. von Roedern, P.G. Clem, R.J. Hanrahan Jr., Mater. Lett. 59 (2005) 1085–1088.
[9] A. Faldt, P.O. Nilsson, J. Phys. F: Met. Phys. 10 (1980) 2573–2580.
[10] W. Siekhaus, A. Nelson, Materials Research Society Fall 2005, Boston, MA, United States. November 28, 2005 trough December 2, 2005. UCRL-PROC-217595.
[11] S. Lin, X. Lai, X. Lv, H. Zhang, Surf. Interf. Anal. 40 (2008) 645–648.
[12] J.P. Crocombette, F. Jollet, L.T. Nga, T. Petit, Phys. Rev. B 6410 (2001) 104107:1.
[13] M. Freyss, T. Petit, J.P. Crocombette, J. Nucl. Mater. 347 (2005) 44.
[14] T. Petit, C. Lemaignan, F. Jollet, B. Bigot, A. Pasturel, Philos. Mag. B 77 (1998) 779.
[15] M. Iwasawa, Y. Chen, Y. Kaneta, T. Ohnuma, H.Y. Geng, M. Kinoshita, Mater. Trans. 47 (2006) 2651.
[16] F. Gupta, G. Brillant, A. Pasturel, Philos. Mag. 87 (2007) 2561.
[17] P. Nerikar, T. Watanabe, J.S. Tulenko, S.R. Phillpot, S.B. Sinnott, J. Nucl. Mater. 384 (2009) 61–69.
[18] D. Gryaznov, E. Heifets, R. Kotomin, Phys. Chem. Chem. Phys. 11 (2009) 7241–7247.
[19] I.D. Prodan, G.E. Scuseria, R.L. Martin, Phys. Rev. B 73 (2006) 045104.
[20] M.D. Segall, P.J.D. Lindan, M.J. Probert, C.J. Pickard, P.J. Hasnip, S.J. Clark, M.C. Payne, J. Phys.: Condens. Matter. 14 (2002) 2717.

[21] A.E. Mattsson, P.A. Schultz, M.P. Desjarlais, T.R. Mattsson, K. Leung, Model. Sim. Mater. Sci. Eng. 13 (2005) R1.
[22] S.L. Dudarev, G.A. Botton, S.Y. Savrasov, Z. Szotek, W.M. Temmerman, A.P. Sutton, Phys. Stat. Sol. (a) 166 (1998) 429.
[23] V.I. Anisimov, F. Aryasetiawa, A.I. Lichtenstein, J. Phys.: Condens. Matter. 9 (1997) 767.
[24] N.J. Mosey, E.A. Carter, Phys. Rev. B 76 (2007) 155123.
[25] P. Villars, L.D. Calvert (Eds.), Person's Handbook of Crystallographic Data for Intermetallic Phases, Metals Park, Ohio, ASM, 1985.
[26] G. Puddu, Eur. Phys. J. A 39 (2009) 335–340.
[27] S.Saha, T.P. Sinha, A. Mookerjee, Phys. Rev. B 62 (2000) 8828.
[28] Q. Chen, X. Lai, B. Bai, M. Chu, Appl. Surf. Sci. 256 (2009) 3047–3050.
[29] P. Nozieres, Phys. Rev. Lett. 8 (1959) 1.